

This document is downloaded from DR-NTU, Nanyang Technological University Library, Singapore.

Title	Constitutive behaviour of high strength concrete under dynamic loads
Author(s)	Li, Bing.; Park, R.; Tanaka, H.
Citation	Li, B., Park, R., & Tanaka, H. (2000). Constitutive behaviour of high strength concrete under dynamic loads. ACI Structural Journal, 97(4), 619-629.
Date	2000
URL	http://hdl.handle.net/10220/8373
Rights	© 2000 American Concrete Institute. This paper was published in ACI structural journal and is made available as an electronic reprint (preprint) with permission of American Concrete Institute. The paper can be found at the following official URL: [http://www.concrete.org/PUBS/JOURNALS/OLJDetails.asp?Home=SJ&ID=7427]. One print or electronic copy may be made for personal use only. Systematic or multiple reproduction, distribution to multiple locations via electronic or other means, duplication of any material in this paper for a fee or for commercial purposes, or modification of the content of the paper is prohibited and is subject to penalties under law.

Constitutive Behavior of High-Strength Concrete under Dynamic Loads

by Li Bing, R. Park, and H. Tanaka

An experimental investigation into the behavior of short reinforced high-strength concrete columns is described. Thirty reinforced concrete columns, either 240 mm diameter circular or 240 mm square and 720 mm high, containing different confining reinforcement configurations, yield strengths of transverse reinforcement, and concrete compressive strengths, were subjected to concentric loads to failure at different strain rates. Results presented include an assessment of the effect of strain rate, different concrete compressive strength, amount and distribution of longitudinal steel, and amount of distribution of transverse steel. A stress-strain curve for confined high-strength concrete loaded at a high strain rate (comparable with seismic loading) is proposed and compared with the curve based on tests conducted at low strain rates.

Keywords: column; high-strength concrete; reinforced concrete; reinforcement; stain; stress.

INTRODUCTION

During severe earthquake ground motion, cyclic loading with high strain rates is imposed on a structure. It was predicted that for a very rigid structure with a short fundamental period of approximately 0.1 s, the rate of straining at some critical regions could be as high as 0.025 per s.¹ To calculate the seismic resistance of the structure, the constitutive relationship of concrete and steel over a wide range of strain rates is required. The effect of high rate on the behavior of plain and confined concrete has received much attention from many researchers. These studies are essentially limited to normal strength concrete with f'_c ranging from 20 to 40 MPa, and normal yield strength reinforcement (f_{yh} less than 500 MPa). Extensive research conducted by Scott et al.,² Soroushian et al.,³ Mander et al.,⁴ Fu et al.,^{5,6} and Dodd and Cooke⁷ investigated the effect of strain rate on the behavior of normal strength concrete. They all found that as the strain rate increased: 1) the compressive strength, secant modulus of elasticity, and slope of the descending branch in the concrete stress-strain curve all increase; and 2) the maximum strain at failure decreases while the strain at maximum stress might decrease or increase, depending on the rate of straining.

With the possible increased utilization of high-strength concrete together with high yield strength of reinforcement for general structural applications, a concern is whether the current understanding of normal strength concrete under high strain rate is applicable to high-strength concrete under high strain rate. Limited information^{5,6} is available on the behavior of high-strength concrete under high strain rates, such as those that would be experienced during earthquakes. There is no detailed technical information available in the two major state-of-the-art reports on high-strength concrete published by ACI Committee 363 ("High-Strength Concrete")⁸ and FIP/CEB.⁹ This paper presents the results of an investigation in which a range of semi-full-size specimens

were tested under conditions that simulated seismic conditions. Thirty reinforced high-strength concrete columns (f'_{co} ranging from 52 to 82.5 MPa) with concrete cover and longitudinal and transverse reinforcement, were subjected to concentric loading to failure at different strain rates. Full details of the tests were reported elsewhere by Li Bing et al.¹⁰

EXPERIMENTAL PROGRAM

To obtain some information about the behavior of confined high-strength concrete under dynamic loading, three different unconfined concrete compressive strengths were selected: 52; 76; and 82.5 MPa. Both square and circular section shapes were selected, both being common in practice. Two different types of reinforcement were used: Grade 430 normal yield strength, and Ulbon high yield strength. Based on the consideration that the axial compression load was limited by the capacity of the testing machine used, which can produce 10 MN in compression, a column section width or diameter of 240 mm was chosen. A cover thickness of 15 mm to the outside of the hoops or spirals was adopted to minimize the influence of the concrete cover and concentrate the investigation on the confined core concrete. To obtain a uniform stress distribution in the central region of the column, which was the instrumented test region, the aspect ratio was made as 3 to 1. Figure 1 and 2 show the test specimens.

TEST SETUP AND INSTRUMENTATION

Concentric vertical loading was provided by a 10 MN electrohydraulic universal testing machine (shown in Fig. 3). The steel reaction columns of the testing machine are stiff enough to permit the machine to measure the descending

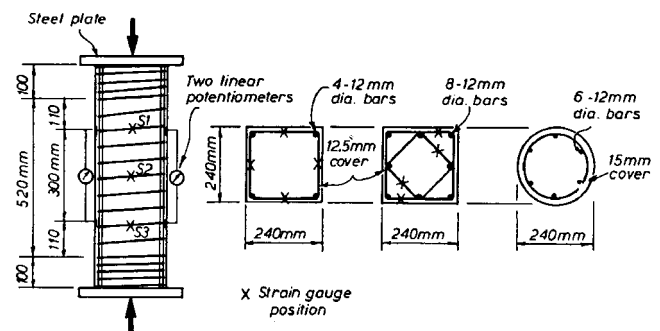


Fig. 1—Short column with axial compressive loading: principal dimensions; test setup; instrumentation; and position of strain gages.

ACI Structural Journal, V. 97, No. 4, July-August 2000.
MS No. 99-167 received August 11, 1998, and reviewed under Institute publication policies. Copyright © 2000, American Concrete Institute. All rights reserved, including the making of copies unless permission is obtained from the copyright proprietors. Pertinent discussion will be published in the May-June 2001 ACI Structural Journal if received by January 1, 2001.

Li Bing is an assistant professor in the School of Civil and Environmental Engineering at Nanyang Technological University, Singapore. He received his BE from Tong Ji University, China, and his PhD from the University of Canterbury, New Zealand. His research interests include reinforced concrete and high-strength concrete structures, particularly design for earthquake resistance and blast loading.

R. Park, F.A.C.I., is an Emeritus professor of civil engineering at the University of Canterbury. He was the coreipient of ACI's Raymond C. Reese Research Award in 1984 and 1989. His research interests include reinforced and prestressed concrete structures, particularly in design and earthquake resistance.

H. Tanaka is an associate professor in the Department of Architecture and Civil Engineering at Toyohashi University of Technology, Japan. He received his BE and ME from Kyoto University, Japan, and his PhD in civil engineering from the University of Canterbury. His research interests include reinforced concrete and high-strength concrete structures, particularly design for earthquake resistance.

branch of the load-strain curve of the test specimens. The tests were conducted at a controlled rate of longitudinal compressive strain of 0.0167/s. The high strain rate adopted could be regarded as indicative of the strain rate expected during the response of reinforced concrete to earthquakes.

The longitudinal concrete strains in the test units were measured using two methods. The first method used the displacement of the ram of the machine to give the overall shortening of the test unit; this displacement was divided by the height of the test unit; this second method used different gage length linear potentiometers to measure the axial strain of the specimen. Two 50 mm linear potentiometers were used to measure strains over the anticipated failure regions (central part of the specimen) over a gage length of approximately 300 mm. Two other linear potentiometers were used to measure strains over length of the specimen (a 640 mm gage). If the diagonal shear plane was formed, this larger gage length could be used instead of the gage length over the central part of the specimen.

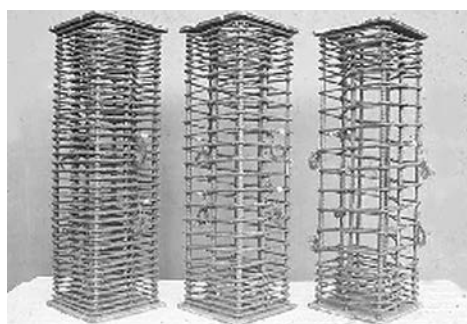
Electrical resistance strain gages were attached to the inside and outside of the transverse hoop bars and helixes at two or three levels within the central part of specimens.

MATERIALS AND TEST UNITS

A local ready-mix plant supplied the high-strength concrete used for the test units. The mixture details are shown in Table 1. The measured slumps of the concrete were all approximately 120 mm. Typical stress-strain curves of reinforcement used are shown in Fig 4. Details of the test units are shown in Table 2 and 3.

TEST PROCEDURE

At the beginning, one specimen was tested at a low rate of strain of 0.000011/s to obtain information for comparison with other specimens tested at a rapid strain rate. All subsequent columns were tested at a rapid strain. To obtain the



rapid strain rate, the stroke control of the testing machine was set to give an average strain rate of 0.0167/s.

TEST OBSERVATIONS

Unconfined high-strength concrete

The unconfined concrete cylinders and prisms of the same size as the reinforced specimens, when tested dynamically at the high strain rate, were observed to form fine vertical microcracks before reaching the maximum load. After the maximum load was reached, a large inclined crack formed that led to a very explosive type of failure. The diagonal failure plane developed at an angle of approximately 65 degrees to the horizontal, as shown in Fig. 5. By comparison, normal strength concrete normally undergoes a more gentle failure, as observed in the tests by Scott et al.² and Mander et al.⁴

Confined high-strength concrete

There was no significant difference in the behavior observed for these confined high-strength concrete specimens and the confined normal strength concrete specimens that Scott et al. and Mander et al. tested.

A diagonal failure plane was found to be a feature of columns with relatively low confinement. This is the result of: 1) insufficient transverse reinforcement to prevent sliding occurring along an inclined failure surface; and 2) the eccentricity caused by uneven spalling of cover concrete. For columns with a low level of confinement, the peak core stress was always reached before spalling was completed, and the eccentricity initially caused the failure to concentrate at one face of the column. The cracks subsequently propagated along a surface of weakness to form a diagonal failure plane. The effectiveness of a given quantity of confinement gradually reduced with increasing concrete compressive strength. Therefore, for a certain concrete compressive strength, a minimum amount of confinement is needed to ensure desirable behavior under dynamic loading. Figure 6 shows that just subsequent to peak load, at $t = 0.7$ s, an inclined crack

Table 1—Mixture proportions for different compressive strengths of concrete

Contents	Weight, kg/m ³		
	52 MPa	75 MPa	82.5 MPa
13 mm aggregate	1150 kg	1188 kg	1188 kg
Kaipoi sand	600 kg	495 kg	495 kg
Yaldhurst sand	150 kg	124 kg	124 kg
Ordinary portland cement	400 kg	400 kg	410 kg
Superplasticizer	2 L	2.5 kg	2.5 L
Water	160 L	138 L	138 L
Silica fume solid	—	40 kg	40 kg
w/c	0.40	0.345	0.337

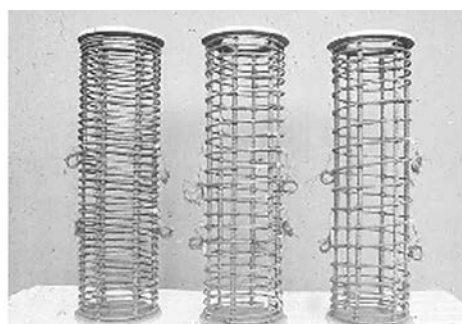


Fig. 2—Typical reinforcement cages for concrete prisms and cylinders.

rapidly developed, and crushing of the cover concrete was more severe at the ends of the diagonal plane. The cover concrete spalled off as relatively large lumps of concrete.

For columns with a relatively large amount of confining steel, the column failure mode gradually changed from diagonal failure to random failure. For columns with high confine-

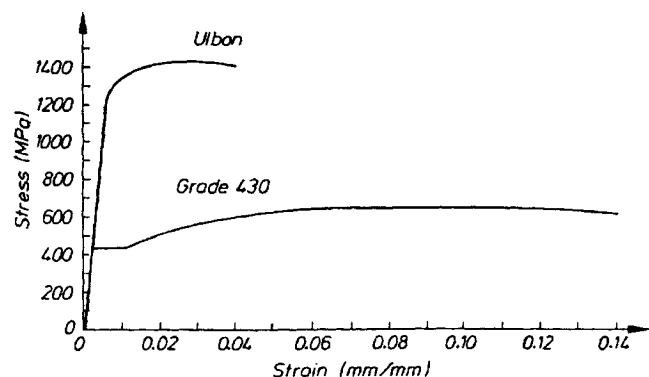


Fig. 3—Typical stress-strain curves for Grade 430 and high-strength reinforcing steel.

ment, the peak stress was always reached after spalling completed. Therefore, the failure concentration upon the surface tended to be random in location and inclination, with no distinct formation of a failure plane. Figure 7 shows that vertical cracks developed very symmetrically in this specimen, and the cover concrete spalled off as large lumps. By $t = 2.10$ s, fracture of some parts of the helixes had occurred, leading to a large explosive failure. It was often found that after testing, the rig, which connected the potentiometers, had inclined to one side. This phenomenon indicates that initially plane sections did not remain plane during the duration of the test. This occurred despite the fact that the end sections remained plane and parallel. This may have been due to very high, localized strains associated with longitudinal bar buckling, which caused local section distortion. As this happened towards the end of testing, however, any errors in measured longitudinal strain would not have been large.

DISCUSSION OF TEST RESULTS

Behavior of unconfined high-strength concrete

The concrete compressive strength is sensitive to variations of strain rate. All of the test results in the literature in-

Table 2—Test specimen properties for square test units

Unit number	f'_{co} , MPa	Strain rate per s	Longitudinal reinforcement			Transverse reinforcement			
			Number of bars	Diameter, mm	f_y , MPa	Diameter, mm	Spacing, mm	f_{yh} , MPa	ρ_s
1C	75.0	0.0167	4	12	443	6	20	445	2.63%
1B	75.0	0.000011	4	12	443	6	20	445	2.63%
2C	75.0	0.0167	8	12	443	6	20	445	4.48%
2B	75.0	0.000011	8	12	443	6	20	445	4.48%
4C	75.0	0.0167	4	12	443	6	35	445	1.50%
4B	75.0	0.000011	4	12	443	6	35	445	1.50%
5C	75.0	0.0167	8	12	443	6	35	445	2.56%
5B	75.0	0.000011	8	12	443	6	35	445	2.56%
7C	75.0	0.0167	4	12	443	6	50	445	1.05%
7B	75.0	0.000011	4	12	443	6	50	445	1.05%
8C	75.0	0.0167	8	12	443	6	50	445	1.79%
8B	75.0	0.000011	8	12	443	6	50	445	1.79%
10C	75.0	0.0167	4	12	443	6	65	445	0.08%
10B	75.0	0.000011	4	12	443	6	65	445	0.08%
11C	75.0	0.0167	8	12	443	6	65	445	1.38%
11B	75.0	0.000011	8	12	443	6	65	445	1.38%
3HB2	52.0	0.0167	8	12	443	6.4	35	1318	2.86%
3HB1	52.0	0.000011	8	12	443	6.4	35	1318	2.86%
1HC2	82.5	0.0167	8	12	443	6.4	20	1318	5.00%
1HC1	82.5	0.000011	8	12	443	6.4	20	1318	5.00%
3HC2	82.5	0.0167	8	12	443	6.4	35	1318	2.86%
3HC1	82.5	0.000011	8	12	443	6.4	35	1318	2.86%

Table 3—Test specimen properties for circular test units

Unit number	f'_{co} , MPa	Strain rate per s	Longitudinal reinforcement			Transverse reinforcement			
			Number of bars	Diameter, mm	f_y , MPa	Diameter, mm	Spacing, mm	f_{yh} , MPa	ρ_s
6C	75.0	0.0167	6	12	443	6	35	445	1.53%
6B	75.0	0.000011	6	12	443	6	35	445	1.53%
12C	75.0	0.0167	6	12	443	6	65	445	0.82%
12B	75.0	0.000011	6	12	443	6	65	445	0.82%
4HB2	75.0	0.0167	6	12	443	6.4	35	1318	1.68%
4HB1	75.0	0.000011	6	12	443	6.4	35	1318	1.68%
2HC2	75.0	0.0167	6	12	443	6.4	65	1318	2.94%
2HC1	75.0	0.000011	6	12	443	6.4	65	1318	2.94%

dicating that the strength of concrete increases as the strain rate increases. The magnitude of the enhancement seems to be linked to moisture content and the extent of cracking within the concrete. The strength of wet concrete is relatively more sensitive to a change in strain rates than dry concrete. The higher the concrete compressive strength, the less sensitive the concrete strength is to strain rate. Based on Dodd and Cooke's⁷ review, strength enhancement from dynamic loading should either be ignored or considered constant. If a constant dynamic magnification factor is to be chosen, a value of 1.2 could be used assuming a strain rate of 0.001 to 0.01 per s.

To verify the previously cited assumption for high-strength concrete, an additional 16 plain cylinders with 200 x 100 mm diameter of two strengths were studied at strain rate ranging from 0.000004 to 0.01/s. The concrete compressive strength under static loading was either $f'_{co} = 58$ or 75 MPa. It was found that the compressive strength increased with increasing strain rate, but the rate of increase of strength of these two

concrete mixtures under dynamic loading was quite different. For $f'_{co} = 58$ MPa, the increase in compressive strength due to dynamic loading at the strain rate of 0.01/s was found to be 58%. For concrete with $f'_{co} = 75$ MPa, only a 13% increase was observed. It can be concluded that high strain rate appears to have a less profound effect on the compressive strength of high-strength concrete.

In the past, some equations for the strength magnification factor D_f of unconfined high-strength concrete have been proposed.

Mander et al.⁴ proposed a D_f based on the results of Watstein¹¹

$$D_f = \frac{1 + \left[\frac{\epsilon}{0.035(f'_{co})} \right]^{\frac{1}{6}}}{1 + \left[\frac{0.000001}{0.035(f'_{co})^2} \right]^{\frac{1}{6}}} \quad (1)$$

Ahmad and Shah¹² proposed a D_f based on their test results

$$D_f = \left[0.95 + 1.86 \frac{\log(\epsilon)}{f'_{co}} \right] \alpha \quad (2)$$

where

ϵ = strain rate in microstrain per s; and
 α = $0.85 + 0.004(d) - 0.008(h)$ for $h/d \geq 5$.

Dilger et al.¹³ proposed a simple unified D_f that does not account for the concrete compressive strength

$$D_f = K_1 + K_2 \log(\epsilon) \quad (3)$$

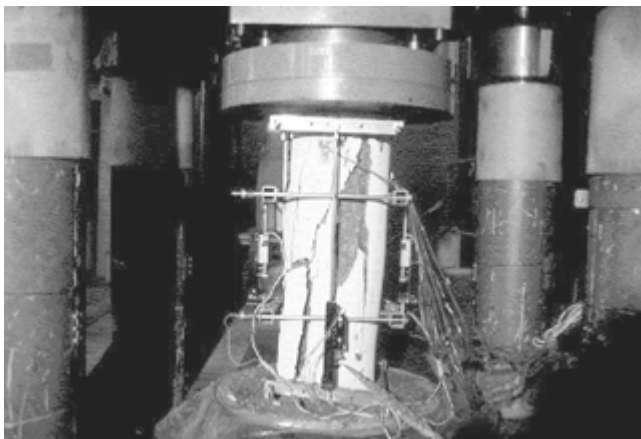


Fig. 4—Test unit setup in testing machine.

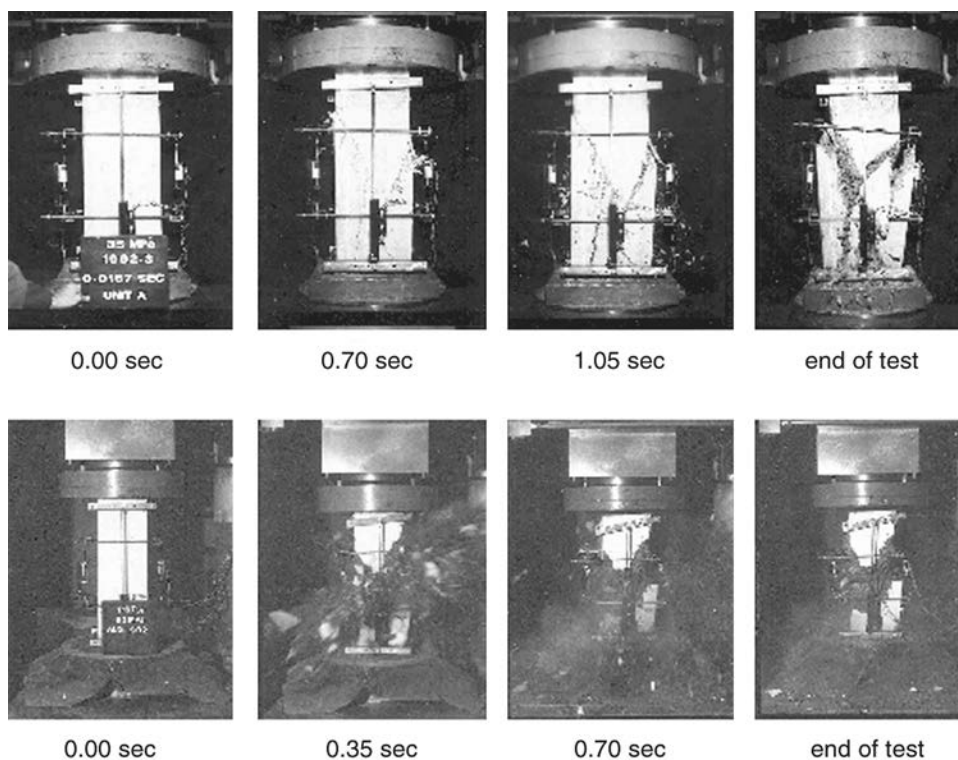


Fig. 5—Test sequence of normal ($f'_{co} = 35$ MPa) and high- ($f'_{co} = 83$ MPa) strength unconfined concrete units at the high strain rates (0.0167/s).

where

ϵ = strain rate in mm/mm per s;

$K_1 = 1.14$ and $K_2 = 0.03$ for $\epsilon < 16 \mu \epsilon/s$; and

$K_1 = 1.38$ and $K_2 = 0.08$ for $\epsilon > 16 \mu \epsilon/s$.

Soroushian et al.³ presents a D_f based on previous work by Scott et al.² and Dilger et al.¹³ The D_f is also independent of the concrete compressive strength, but the effect of the moisture content was considered

$$D_f = K_1 + K_2 \log(\epsilon) + K_3 (\log(\epsilon))^2 \quad (4)$$

where

$K_1 = 1.48$, $K_2 = 0.206$, and $K_3 = 0.0221$ for dry concrete;

$K_1 = 2.54$, $K_2 = 0.580$, and $K_3 = 0.0543$ for wet concrete; and

$K_1 = 1.48$, $K_2 = 0.160$, and $K_3 = 0.0127$ for all concrete.

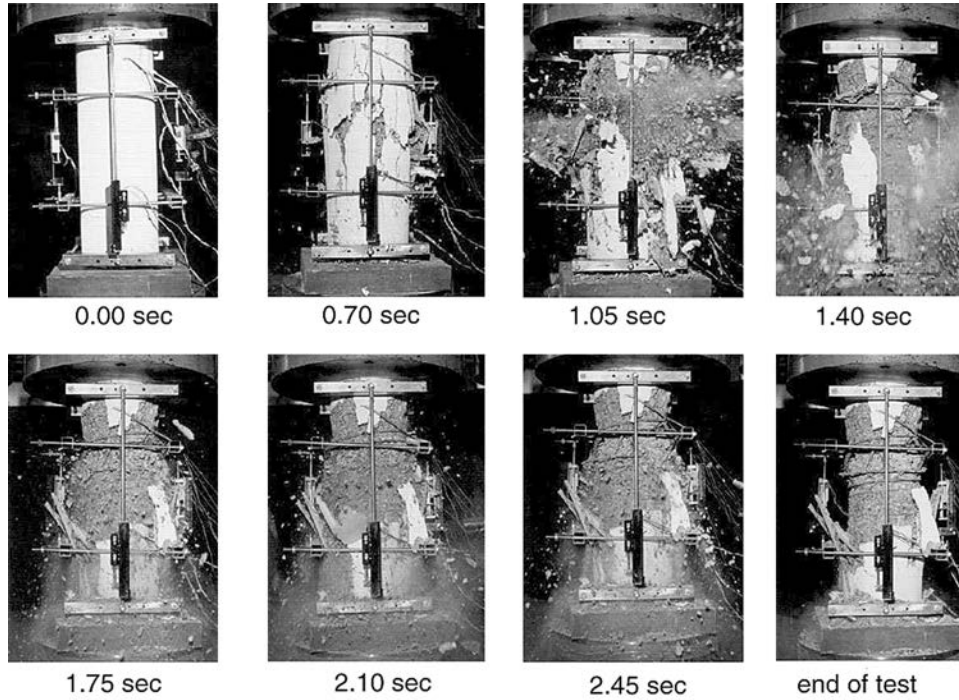


Fig. 6—Photographs showing test sequence of high-strength concrete unit with high yield strength rectilinear confinement at high strain rate (0.0167/s).

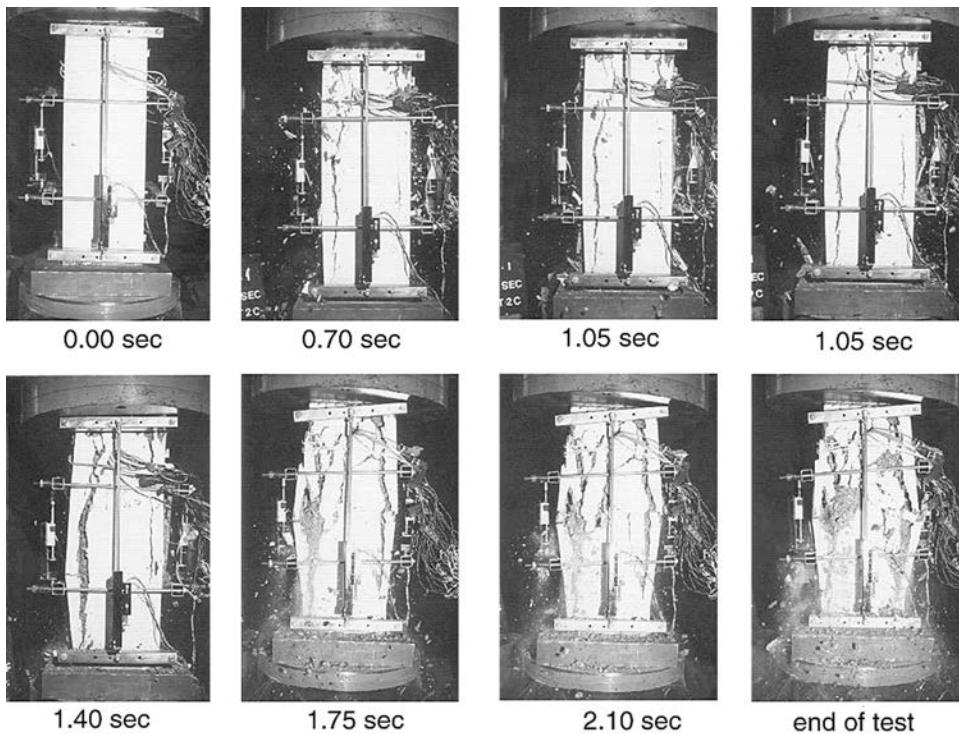


Fig. 7—Photographs showing test sequence of high-strength concrete unit with normal yield strength rectilinear confinement at the high strain rate (0.0167/s).

The test results for different f'_{co} are compared with the D_f proposed by different researchers. For moderate f'_{co} , the results are not in good agreement with the D_f proposed by different researchers. For high f'_{co} , the D_f proposed by Mander et al.⁴ and Ahmad and Shah¹² provides a reasonably accurate prediction.

Many researchers have found that the curing condition determines the magnitude of the effect of strain rate on the compressive strength of concrete. Kaplan¹⁴ tested a large number of concrete prisms and cylinders to investigate the relationship between concrete strength and loading rate for concrete with various moisture contents and curing conditions. Kaplan concluded that the moisture content of concrete is one of the principle variables affecting the relationship between strength and loading rate. In this current study, it was found that in the case of high-strength concrete, the strain rate effect is not as sensitive to the curing condition as for normal strength concrete. There was no observed difference in behavior between two cylinders with different curing conditions; one was just out of the fog room, and other had been dried in the air for 3 days, when tested under the high strain rate of 0.01/s.

Behavior of confined high-strength concrete

Scott et al.² tested a total of 20 reinforced normal strength concrete specimens of identical dimensions (450 x 450 x 1200 mm) with different longitudinal and transverse reinforcement configurations. The test results indicated significant increases in the compressive strength of the concrete core as the strain rate was increased. Also, the maximum concrete core stress and strain at failure both increased as a result of better confinement of the concrete core that was provided by an increase in the volumetric ratio of transverse reinforcement ρ_s .

In the current study, a total of 30 specimens were tested. The B series of test units was loaded at a low strain rate, and the C series of test units was loaded at a high strain rate. Table 4 and 5 list the test results for square and circular section test units.

Effect of confinement ratio—From Table 4 and 5, it is evident that for confined normal and high-strength concrete under dynamic loading condition, an increase in the confinement ratio increased the maximum core concrete stress f'_{cc} attained by up to 20% and decreased the slope of the descending branch of stress-strain curve. An increase in hoop or spiral spacing tended to reduce the efficiency of the confinement. High-strength concrete specimens appeared to be

Table 4—Details of test results for square section units

Unit number	f'_{co} , MPa	E_c , MPa	D_E	f'_{cc} , MPa	D_f	ϵ'_{cc}	D_ϵ
1C	75.0	45,766	1.29	99.12	1.17	0.0056	0.93
1B	75.0	35,430	1.00	84.76	1.00	0.0060	1.00
2C	75.0	34,283	0.97	117.2	1.09	0.0078	1.08
2B	75.0	35,429	1.00	107.4	1.00	0.0072	1.00
4C	75.0	31,700	1.37	87.78	1.08	0.0035	0.88
4B	75.0	23,118	1.00	81.23	1.00	0.0040	1.00
5C	75.0	33,291	0.98	97.17	1.20	0.0054	1.04
5B	75.0	35,429	1.00	81.04	1.00	0.0052	1.00
7C	75.0	34,515	0.97	82.21	0.98	0.0034	0.88
7B	75.0	35,429	1.00	84.22	1.00	0.0038	1.00
8C	75.0	34,191	1.11	91.17	1.13	0.0060	1.10
8B	75.0	30,931	1.00	80.48	1.00	0.0055	1.00
10C	75.0	32,329	0.91	79.38	1.09	0.0026	1.00
10B	75.0	35,429	1.00	73.12	1.00	0.0026	1.00
11C	75.0	30,235	1.03	81.63	1.08	0.0042	0.98
11B	75.0	29,413	1.00	75.83	1.00	0.0043	1.00
3HB2	52.0	29,375	1.06	79.41	0.97	0.0181	0.60
3HB1	52.0	27,664	1.00	81.71	1.00	0.0300	1.00
1HC2	82.5	36,419	1.09	149.9	1.00	0.0145	0.73
1HC1	82.5	33,297	1.00	149.3	1.00	0.0200	1.00
3HC2	82.5	38,829	1.29	112.2	1.09	0.0038	0.24
3HC1	82.5	30,202	1.00	103.2	1.00	0.0160	1.00

Table 5—Details of test results for circular section units

Unit number	f'_{co} , MPa	E_c , MPa	D_E	f'_{cc} , MPa	D_f	ϵ'_{cc}	D_ϵ
6C	75.0	42,926	1.29	108.8	1.17	0.0054	1.04
6B	75.0	33,233	1.00	92.7	1.00	0.0052	1.00
12C	75.0	28,854	0.88	81.16	1.25	0.0032	1.60
12B	75.0	32,708	1.00	64.74	1.00	0.0020	1.00
4HB2	52.0	29,256	1.02	86.40	0.98	0.0121	0.61
4HB1	52.0	28,775	1.00	87.6	1.00	0.0200	1.00
2HC2	82.5	35,523	1.24	144.5	0.99	0.0130	0.93
2HC1	82.5	28,423	1.00	145.3	1.00	0.0140	1.00

much more sensitive to changes in the confinement ratio than normal strength concrete specimens.

Effect of strain rate—For high-strength concrete specimens confined by normal yield strength steel, an increase in the rate of strain to 0.0167/s resulted in approximately an 11% increase in the maximum concrete core stress f'_{cc} . The average values taken from strain gages that were reading at the same level indicated that the normal yield strength steel was very close to or barely greater than the strain at the yield of the transverse reinforcement. This finding is independent of concrete compressive strength. Hence, it can be concluded that it is reasonable to take the normal yield strength of the transverse steel when calculating the confining stress. This increase in the peak stress during the high strain rate is approximately 50% smaller; the increase in the peak stress in normal strength concrete was approximately 25%, predicted by Scott.²

For specimens confined by high yield strength steel, an increase in the rate of strain did not result in a significant increase in the maximum concrete stress f'_{cc} . When the peak strength of the confined concrete is reached, the average value of the strain gages reading at the same level was always less than the strain at the commencement of yield of the high yield strength steel. This indicates that full confinement is delayed and hence, its main contribution is that it maintains the ductility, but the strength gain may be much smaller. Therefore, the full high yield strength steel can not be used when calculating the confining stress. Also, it seems that change in section shape from circular to square had no obvious effect.

Hence, although some strength enhancement was observed in the dynamic tests, it was evident that the effect of dynamic loading on concrete compressive strength reduces when high-strength concrete is used. Dodd and Cooke⁷ have suggested that strength enhancement due to dynamic loading should be either ignored or considered constant. Based on this study, if a constant magnification factor is to be chosen, a value of 1.1, assuming a high strain rate of up to 0.01, could be used for high-strength concrete confined by normal yield strength steel. A dynamic magnification factor of 1.0 is suggested for high-strength concrete confined by high yield strength steel.

Effect of strain rate on strain at peak stress D_ϵ

In the literature, there is no agreement about the effect of strain rate on the corresponding strain at peak stress. Different researchers have proposed contradictory trends. This may be the result of different gage lengths used by different researchers. In this study, for high-strength concrete confined by normal yield strength steel, the effect of strain rate on the strain at the peak stress was very small. For high-strength concrete confined by high yield strength steel, however, a large decrease in the strain at the peak stress was observed at high strain rates. This decrease was as much as 35%.

There are two main causes for reduction in strain at peak stress for high-strength concrete confined by high yield strength steel. First, time available for internal microcracking development or propagation is significantly reduced during high strain rate loading. Second, the presence of high yield strength confinement reinforcement greatly prevents excessive growth of the internal microcracking and stimulates the nucleation of those cracks. Hence, based on these test results, it is suggested that the strain rate should be considered to have no effect on the strain at peak stress for high-strength concrete confined by normal yield strength steel. For high-strength concrete confined by high yield strength

steel, the modification factor for the strain at peak stress due to dynamic effect D_ϵ can be assumed to be 0.65.

Effect of strain rate on stiffness enhancement D_E

It was observed that there was a slight increase in the modulus of elasticity with an increase in strain rate, but this increase was much less significant than the corresponding increase in compressive strength of concrete based on previously reported summaries. In this study, it was found that columns with high levels of confinement were much more sensitive to changes in the modulus of elasticity E_c due to high strain rates, than columns with relatively low levels of confinement. For columns confined by normal yield strength steel, it seems that the modulus of elasticity did not change with strain rate. The exceptions were columns confined by high yield strength steel, where an average 13% increase in the modulus of elasticity under dynamic loading was found. Based on test results, it is suggested that the stiffness enhancement factor D_E due to high strain rate for concrete confined by the two different types of confining reinforcement can be taken as 1.1.

Effect of strain rate on trends in stress-strain curve behavior of confined concrete

In general, there were no differences between the behavior of high-strength concrete columns and normal strength concrete columns loaded at different strain rates with respect to trends in the stress-strain curve behavior. An increase in the rate of strain resulted in an increase or maintenance of f'_{cc} , and the modulus of elasticity depended on the level of confinement. The common finding regarding stress-strain curve behavior was an increase in the slope of the descending branch of the stress-strain curve under dynamic loading.

COMPARISON OF TEST RESULTS WITH STRESS-STRAIN CURVE FOR HIGH-STRENGTH CONCRETE

Experiment stress-strain curves for core concrete

The longitudinal load carried by the confined core at a given longitudinal strain can be obtained from the load carried by the column less the load carried by the cover concrete obtained from measured stress-strain curves for the unconfined concrete, and less the load carried by the longitudinal reinforcement as obtained from the measured stress-strain curves for the steel. Then, the stress carried by the confined concrete can be obtained by dividing that load by the area of the concrete core, taken as the area outside of the transverse reinforcement. Comparison of experimental stress-strain curves for the confined concrete of the units for high and low strain rates are shown in Fig. 8, 9, and 10.

Stress-strain curves proposed by Bing et al.¹⁰

Low strain rate—The stress-strain relation for confined high strength concrete, proposed by Bing et al.,¹⁰ was derived from tests with low strain rates. The stress-strain relation of confined concrete is given as follows

when $0 \leq \epsilon_c \leq \epsilon_{cc}$

$$f_{cd} = E_c \epsilon_c + \frac{(f'_{co} - E_c \epsilon_c)}{2} \epsilon_c^2 \quad (5)$$

when $\epsilon_{co} \leq \epsilon_c \leq \epsilon_{cc}$

$$f_c = f'_{cc} - \frac{(f'_{cc} - f'_{co})}{(\epsilon_c - \epsilon_{cc})} \times (\epsilon_c - \epsilon_{cc})^2 \quad (6)$$

when $\epsilon_c > \epsilon_{cc}$

$$f_c = f'_{cc} - \beta \frac{f'_{cc}}{\epsilon_{cc}} \times (\epsilon_c - \epsilon_{cc}) \geq 0.4f'_{cc} \quad (7)$$

High strain rate—On the basis of the observed stress-strain behavior in this study, the stress-strain relation proposed by Bing et al.¹⁰ may be adapted for the high strain rate

by applying multiplying factors to the peak stress, the strain at the peak stress, modulus of elasticity, and the slope of the falling branch. Thus, for the high strain rate, the stress-strain relation is given by the following

when $0 \leq \epsilon_{cd} \leq \epsilon_{ccd}$

$$f_{cd} = E_{cd}\epsilon_{cd} + \frac{(f'_{co} - E_{cd}\epsilon_{cod})}{\epsilon_{cod}^2} \epsilon_{cd}^2 \quad (8)$$

when $\epsilon_{cod} \leq \epsilon_{cd} \leq \epsilon_{ccd}$

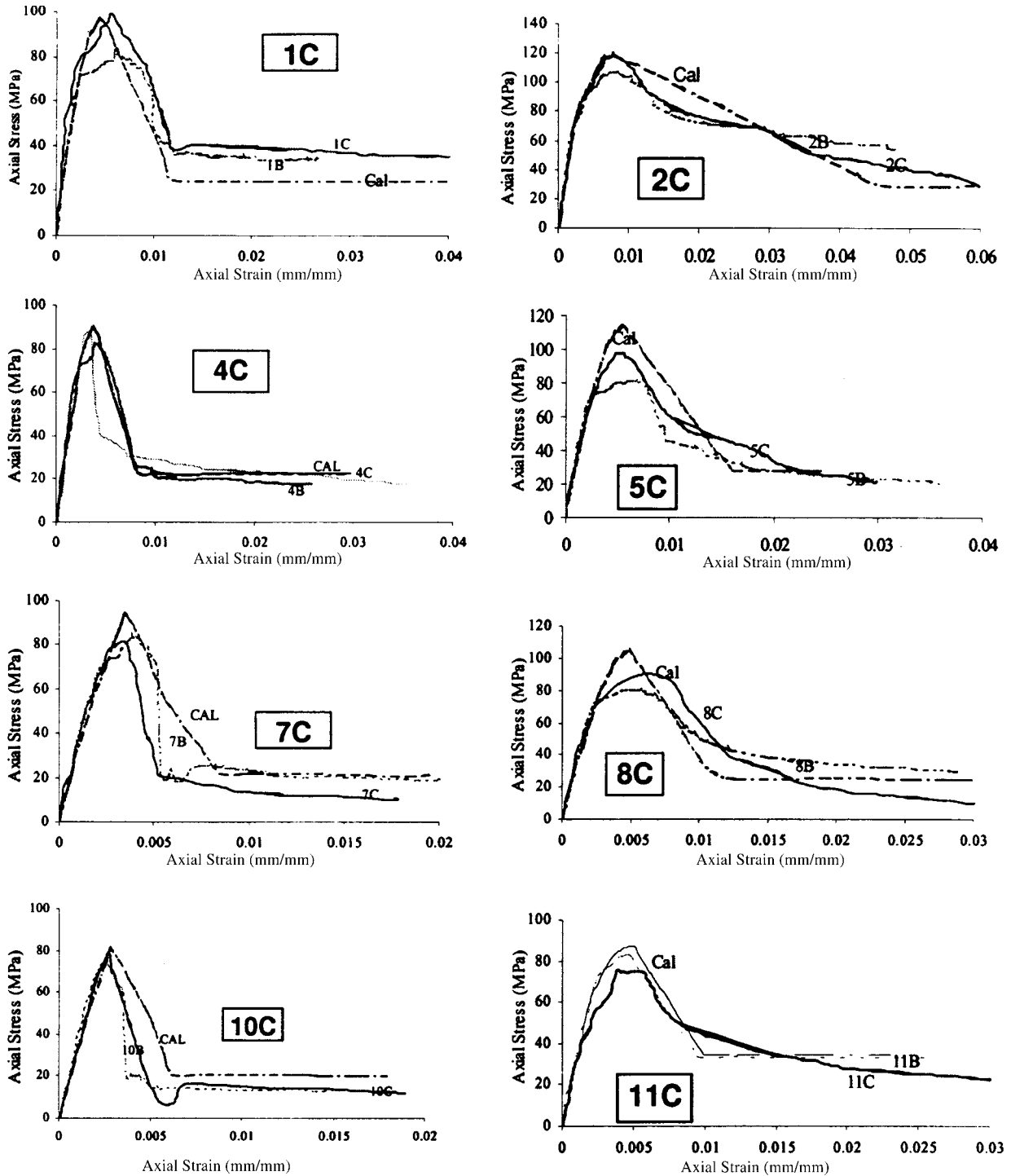


Fig. 8—Comparison of stress-strain curves for core concrete of square core section confined by Grade 430 steel.

$$f_{cd} = f'_{ccd} - \frac{(f'_{ccd} - f'_{cod})}{(\epsilon_{ccd} - \epsilon_{cod})} \times (\epsilon_{cd} - \epsilon_{ccd})^2 \quad (9)$$

when $\epsilon_{cd} > \epsilon_{ccd}$

$$f_{cd} = f'_{ccd} - \beta \frac{f'_{ccd}}{\epsilon_{ccd}} \times (\epsilon_{cd} - \epsilon_{ccd}) \geq 0.25f'_{ccd} \quad (10)$$

where

$$f_{ccd} = D_f f'_{cc};$$

$$E_{cd} = D_E E_c;$$

$$\epsilon_{ccd} = D_\epsilon \epsilon_{cc};$$

$D_f = 1.1$ for high-strength concrete confined by Grade 430 steel;

$D_f = 1.0$ for high-strength concrete confined by high yield strength steel;

$D_E = 1.1$ for high-strength concrete confined by both Grade 430 and high yield strength steel;

$D_\epsilon = 1.0$ for high-strength concrete confined by Grade 430 steel; and

$D_\epsilon = 0.65$ for high-strength concrete confined by high yield strength steel.

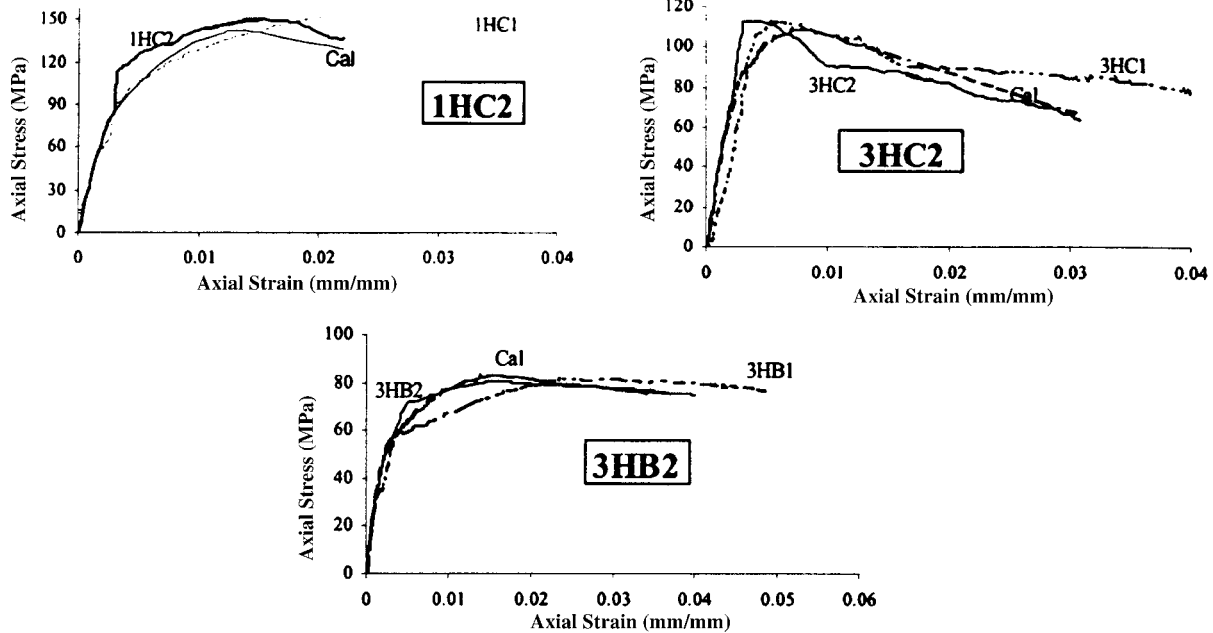


Fig. 9—Comparison of stress-strain curves for core concrete of square cross section confined by high-strength steel ($f_{yh} = 1318$ MPa).

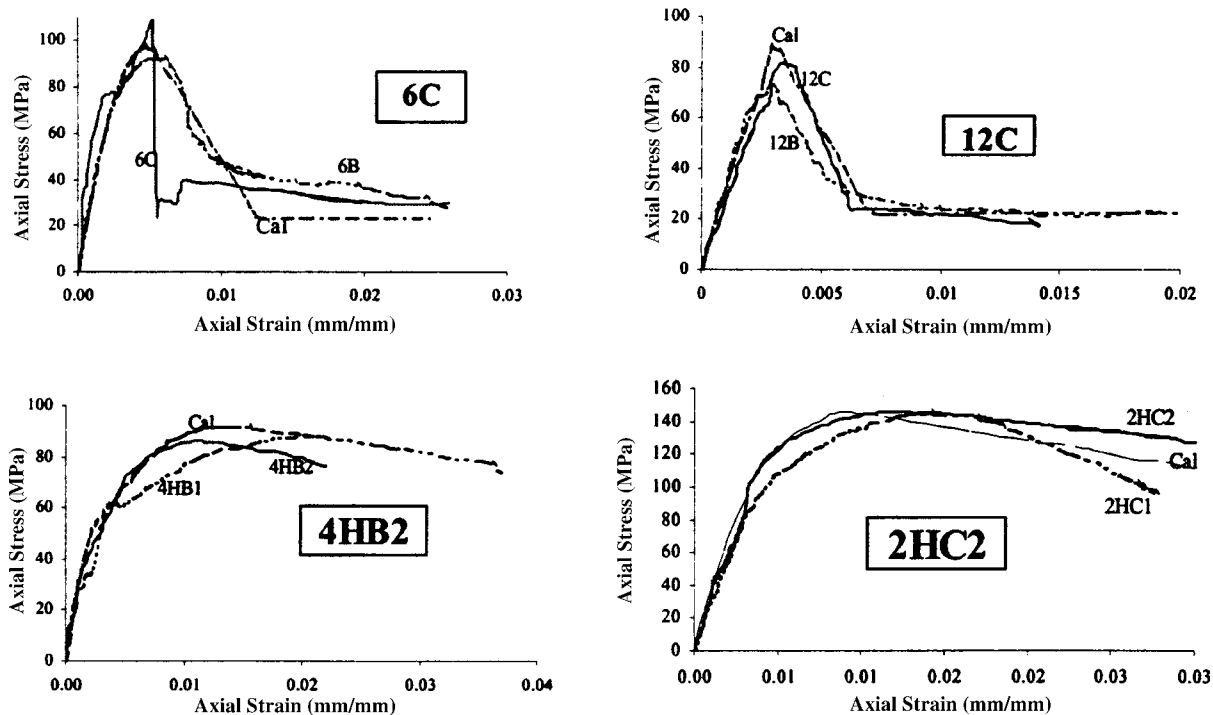


Fig. 10—Comparison of stress-strain curves for core concrete of circular section confined by Grade 430 and high-strength steel ($f_{yh} = 1318$ MPa).

Circular confinement with ordinary strength steel—

$$f'_{cc} = f'_{co} \left[-0.413 + 1.413 \sqrt{1 + 11.4 \frac{f'_l}{f'_{co}} - 2 \frac{f'_l}{f'_{co}}} \right] \quad (11)$$

$$\frac{\epsilon_{cc}}{\epsilon_{co}} = 1.0 + 384 \left(\frac{f'_l}{f'_{co}} \right)^2 \quad (12)$$

$$\frac{\epsilon_{cu}}{\epsilon_{co}} = 2.0 + (143.5 - 1.48f'_{co}) \sqrt{\frac{f'_l}{f'_{co}}} \text{ when } f'_{co} < 80 \text{ MPa} \quad (13)$$

$$\frac{\epsilon_{cu}}{\epsilon_{co}} = 2.0 + (90 - 0.74f'_{co}) \sqrt{\frac{f'_l}{f'_{co}}} \text{ when } f'_{co} \geq 80 \text{ MPa} \quad (14)$$

$$\beta = 0.2 (f_{co} \leq 80 \text{ MPa})$$

Rectilinear confinement with ordinary strength steel—

$$f'_{cc} = f'_{co} \left[-0.413 + 1.413 \sqrt{1 + 11.4 \frac{f'_l}{f'_{co}} - 2 \frac{f'_l}{f'_{co}}} \right] \quad (15)$$

$$\frac{\epsilon_{cc}}{\epsilon_{co}} = 1.0 + 384 \left(\frac{f'_l}{f'_{co}} \right)^2 \quad (16)$$

$$\frac{\epsilon_{cu}}{\epsilon_{co}} = 2.0 + (122.5 - 0.92f'_{co}) \sqrt{\frac{f'_l}{f'_{co}}} \text{ when } f'_{co} < 80 \text{ MPa} \quad (17)$$

$$\frac{\epsilon_{cu}}{\epsilon_{co}} = 2.0 + (82.8 - 0.37f'_{co}) \sqrt{\frac{f'_l}{f'_{co}}} \text{ when } f'_{co} \geq 80 \text{ MPa} \quad (18)$$

Circular confinement with high yield strength steel—

$$f'_{cc} = f'_{co} \left[-1.254 + 2.254 \sqrt{1 + 7.94 \alpha_s \frac{f'_l}{f'_{co}} - 2 \alpha_s \frac{f'_l}{f'_{co}}} \right] \quad (19)$$

$$\alpha_s = (21.2 - 0.35f'_{co}) \frac{f'_l}{f'_{co}} \text{ when } f'_{co} \leq 50 \text{ MPa} \quad (20)$$

$$\alpha_s = 3.1 \frac{f'_l}{f'_{co}} \text{ when } f'_{co} > 50 \text{ MPa} \quad (21)$$

$$\frac{\epsilon_{cc}}{\epsilon_{co}} = 1.0 + (120 - 1.554f'_{co}) \left(\frac{f'_l}{f'_{co}} \right) \text{ when } f'_{co} \leq 50 \text{ MPa} \quad (22)$$

$$\frac{\epsilon_{cc}}{\epsilon_{co}} = 1.0 + (71.4 - 0.623f'_{co}) \left(\frac{f'_l}{f'_{co}} \right) \text{ when } f'_{co} > 50 \text{ MPa} \quad (23)$$

$$\frac{\epsilon_{cu}}{\epsilon_{co}} = 2.0 + (87 - 1.06f'_{co}) \sqrt{\frac{f'_l}{f'_{co}}} \text{ when } f'_{co} \leq 50 \text{ MPa} \quad (24)$$

$$\frac{\epsilon_{cu}}{\epsilon_{co}} = 2.0 + (53.4 - 0.42f'_{co}) \sqrt{\frac{f'_l}{f'_{co}}} \text{ when } f'_{co} > 50 \text{ MPa} \quad (25)$$

$$\beta = 0.2 (f_{co} \leq 80 \text{ MPa})$$

Rectilinear confinement with high-strength steel—

$$f'_{cc} = f'_{co} \left[-1.254 + 2.254 \sqrt{1 + 7.94 \alpha_s \frac{f'_l}{f'_{co}} - 2 \alpha_s \frac{f'_l}{f'_{co}}} \right] \quad (26)$$

$$\alpha_s = 1.56 \left(\frac{f'_l}{f'_{co}} \right) \quad (27)$$

$$\frac{\epsilon_{cc}}{\epsilon_{co}} = 1.0 + (78.1 - 0.83f'_{co}) \left(\frac{f'_l}{f'_{co}} \right) \text{ when } f'_{co} \leq 50 \text{ MPa} \quad (28)$$

$$\frac{\epsilon_{cc}}{\epsilon_{co}} = 1.0 + (55.3 - 0.39f'_{co}) \left(\frac{f'_l}{f'_{co}} \right) \text{ when } f'_{co} > 50 \text{ MPa} \quad (29)$$

$$\frac{\epsilon_{cu}}{\epsilon_{co}} = 2.0 + (70 - 0.6f'_{co}) \sqrt{\frac{f'_l}{f'_{co}}} \text{ when } f'_{co} \leq 50 \text{ MPa} \quad (30)$$

$$\frac{\epsilon_{cu}}{\epsilon_{co}} = 2.0 + (49 - 0.2f'_{co}) \sqrt{\frac{f'_l}{f'_{co}}} \text{ when } f'_{co} > 50 \text{ MPa} \quad (31)$$

$$\beta = 0.2 (f_{co} \leq 80 \text{ MPa})$$

The previously stated analytical model developed in this study was applied to the test results. Figure 8, 9 and 10 show the comparison of the experimental and the proposed analytical curves. It should be noted that the agreement between the analytical and the experimental results is reasonably good. Thus, it is concluded that this model can be used for the calculation of the stress-strain relationship of confined high-strength concrete under dynamic conditions.

CONCLUSIONS

Based on the results of this investigation, the following conclusions may be drawn:

1. The test results confirmed that high strain rates appear to have a less profound effect on the stress-strain relationship of high-strength concrete than on low- and moderate strength concrete;

2. When the concrete compressive strength reached 75 MPa, the compressive strength enhancement due to dynamic loading appeared to become insensitive to the curing condition. Also, the strength enhancement due to dynamic loading became less with increase in concrete compressive strength;

3. For the test units confined by Grade 430 steel, a high strain rate resulted in an almost 11% increase in the concrete core compressive strength, a slight increase in the modulus of elasticity, and an increase in the slope of the descending branch of the stress-strain curve. The effect of strain rate on the strain corresponding to the peak stress was much smaller or nearly insignificant;

4. For the test units confined by high yield steel ($f_{yh} = 1318$ MPa), an increase in the rate of strain may not result in an increase in the concrete core compressive strength, but it

does increase the modulus of elasticity and the slope of the descending branch of the stress-strain curve. A large decrease in the strain at the peak stress was observed;

5. There was no obvious effect of cross-sectional shape on the behavior of the test units in this study; and

6. The proposed analytical stress-strain model for loading conditions with high strain rate was found to give reasonable predictions of the experimental behavior of high-strength test units.

ACKNOWLEDGMENTS

Financial support from the Cement and Concrete Association of New Zealand, the New Zealand Concrete Society, Firth Certified Concrete, Pacific Steel Ltd., Koshuha-Netsuran Co. of Japan, Taisei Corp. of Japan, WG Grace (NZ) Ltd., and the New Zealand Ministry of External Relations and Trade is gratefully acknowledged.

NOTATIONS

d_b	=	nominal diameter of reinforcing bar
D	=	diameter or least lateral dimension of concrete unit
D_E	=	dynamic factor for stiffness magnification
D_f	=	dynamic factor for strength magnification
D_ϵ	=	dynamic factor for strain at peak stress
E_c	=	Young's modulus of elasticity for concrete under static loading
E_{cd}	=	Young's modulus of elasticity for concrete under dynamic loading
E_s	=	Young's modulus of elasticity for steel
f_c	=	concrete stress
f'_{cc}	=	confined concrete compressive strength under static loading
f'_{ccd}	=	confined concrete compressive strength under dynamic loading
f_{cd}	=	concrete stress under dynamic loading
f'_{co}	=	in-place unconfined concrete compressive strength under static loading
f_l	=	transverse confining stress
f_y	=	yield strength of steel in tension
f_{yh}	=	yield strength of transverse reinforcing steel
s_h	=	center-to-center spacing of spiral or hoop sets
ϵ_c	=	concrete compressive strain
ϵ_{cd}	=	concrete compressive strain under dynamic loading
ϵ_{cc}	=	strain at maximum confined strength of concrete f'_{cc} under static loading
ϵ_{ccd}	=	strain at maximum confined strength of concrete f'_{cc} under dynamic loading
ϵ_{co}	=	compressive strain at maximum in-place unconfined concrete strength f'_{co} under static loading
ϵ_{cod}	=	compressive strain at maximum in-place unconfined concrete strength $D_f f'_{co}$ under dynamic loading

ϵ_y	=	yield strain of steel
ρ_s	=	volumetric ratio of confining reinforcement-to-core concrete

REFERENCES

- Bertero, V. V., "Experimental Studies Concerning Reinforced, Prestressed and Partially Prestressed Concrete Structures and Their Elements," *Symposium on Resistant and Ultimate Deformability of Structures Acted on by Well-Defined Repeated Loads*, IABSE, 1972, pp. 67-99.
- Scott, B. D.; Park, R.; and Priestley, M. J. N., "Stress-Strain Relationships for Confined Concrete: Rectangular Sections," *Research Report 80-6*, Department of Civil Engineering, University of Canterbury, New Zealand, Feb. 1980, 105 pp.
- Soroushian, P., and Sim, J., "Axial Behavior of Reinforced Concrete Columns under Dynamic Loading," *ACI Structural Journal*, V. 83, No. 6, Nov.-Dec. 1986, pp. 1018-1025.
- Mander, J. B.; Priestley, M. J. N.; and Park, R., "Seismic Design of Bridge Piers," *Research Report 84-2*, Department of Civil Engineering, University of Canterbury, New Zealand, 1984, 444 pp.
- Fu, H. C.; Erki, M. A.; and Seckin, M., "Review of Effect Loading Rate on Concrete in Compression," *ASCE Journal of Structural Engineering*, V. 117, No. 12, Dec. 1991, pp. 3645-3659.
- Fu, H. C.; Erki, M. A.; and Seckin, M., "Review of Loading Rate on Reinforced Concrete," *ASCE Journal of Structural Engineering*, V. 117, No. 12, Dec. 1991, pp. 3660-3679.
- Dodd, L. L., and Cooke, N., "Dynamic Behavior of Reinforced Concrete Bridge Pier Subjected to New Zealand Seismicity," *Research Report 92-6*, Department of Civil Engineering, University of Canterbury, New Zealand, 1992, 460 pp.
- ACI Committee 363, "State-of-the-Art Report on High-Strength Concrete," *ACI JOURNAL, Proceedings* V. 81, No. 4, July-Aug. 1984, pp. 364-411.
- FIP/CEB, "High-Strength Concrete—State-of-the-Art Report," *SR 90/1 Bulletin 'd Information* No. 197, Aug. 1990, 6 pp.
- Bing, L.; Park, R.; and Tanaka, H., "Strength and Ductility of Reinforced Concrete Members and Frames Constructed Using High-Strength Concrete," *Research Report No. 94-5*, University of Canterbury, New Zealand, 389 pp.
- Watstein, D., "Effect of Straining Rate on Compressive Strength and Elastic Properties of Concrete," *ACI JOURNAL, Proceedings* V. 49, No. 8, 1953, pp. 729-741.
- Ahmad, S. H., and Shah, S. P., "Behavior of Hoop Confined Concrete under High Strain Rate," *ACI JOURNAL, Proceedings* V. 82, No. 5, Sept.-Oct. 1985, pp. 634-647.
- Dilger, W. H.; Koch, R.; and Kowalczyk, R., "Ductility of Plain and Confined Concrete under Different Strain Rates," *ACI JOURNAL, Proceedings* V. 81, No. 1, 1984, pp. 73-81.
- Kaplan, S. A., "Factors Affecting Relationship between Rate of Loading and Measured Compressive Strength of Concrete," *Magazine of Concrete Research*, V. 32, No. 111, pp. 79-88.